ELSEVIER

www.elsevier.nl/locate/jorganchem

Journal of Organometallic Chemistry 622 (2001) 280–285

Journal of Organometallic Chemistry

Syntheses of new ruthenium carbonyl terpyridine *o*-phenylene complexes: strong interaction between carbonyl and *o*-phenylene ligands

Hideki Sugimoto [1], Koji Tanaka *

Institute for Molecular Science, Nishigo-Naka, Okazaki 444-8585, Japan

Received 19 October 2000; received in revised form 7 December 2000; accepted 9 December 2000

Abstract

Ruthenium carbonyl *o*-phenylene complexes, Ru(CO)(3,6-Bu_2seq)(trpy)]PF_6 ([**1**]PF_6) and [Ru(CO)(*o*-monothiocat)(trpy)] (**2**), were prepared by the reaction of [Ru(CO)Cl_2(trpy)] with the corresponding *o*-phenylenes in 2-methoxyethanol. X-ray crystallographic study of [**1**]BF_4 indicated that the ruthenium center is coordinated by carbonyl, three nitrogens of trpy and two oxygens of 3,6-Bu_2seq. ESR of [**1**]PF_6 and **2** indicated that the electronic structures of ruthenium-*o*-phenylene unit of the complexes have Ru(II)-3,6-Bu_2seq and Ru(II)-*o*-monothiocat forms, respectively. Significant differences in the redox behavior and the spectroscopical properties between [**1**]PF_6 and **2** and [RuCl(3,5-Bu_2seq)(trpy)] were ascribed to the strong interaction between *o*-phenylene and carbonyl ligands through Ru(II). © 2001 Elsevier Science B.V. All rights reserved.

Keywords: *o*-Phenylene; Ruthenium; Carbonyl; Electronic structure; Crystal structure

1. Introduction

Dioxolene is non innocent ligand that takes three oxidation states with a wide range of redox potentials (Scheme 1). It is well known that orbital energy levels of the central metals and the ligands are very close in some metal–dioxolene complexes[2].

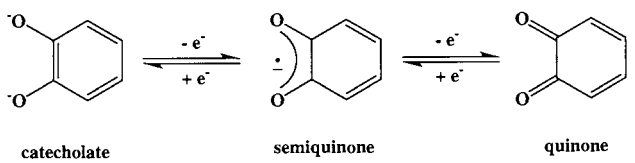

Scheme 1.

These metal complexes are endowed with the inherent multi step redox behavior resulting from the combinations of the oxidation states of the metal and the ligands [1]. Dioxolene ligands are also found in active sites of some metalloproteins, and play a role as redox centers [2]. The 4d and 5d members of the Group 7 and 8 elements, rhenium, ruthenium, and osmium, and radioactive technetium, draw attention because of their versatile redox behavior. Piepont et al. and Lever et al. have extensively studied ruthenium–dioxolene complexes [3]. The feature of the complexes is a large electron delocalization between dπ–pπ orbitals of ruthenium and dioxolene ligands, where the extent of the electron distribution is very sensitive to the orbital energy levels of the metal and the ligands. Reversible electrochemical redox processes and the characteristic electronic spectra depending on their oxidation states were observed in a series of complexes of [Ru(dioxolene)$(bpy)_2]^{n+}$ and [Ru(dioxolene)$_2$(bpy)]$^{n+}$ [4a,e,f]. Recently, we reported ruthenium–dioxolene complexes ([RuX(dioxolene)(trpy)]$^{n+}$) with a substitution labile ligand X such as Cl^-, CH_3COO^-, H_2O aimed at activation of small molecules by taking advantage of the characteristic redox behavior [4,5]. On the other

* Corresponding author. Fax: +81-564-555245.
E-mail address: ktanaka@ims.ac.jp (K. Tanaka).

[1] Present address. Department of Chemistry, Graduate School of Science, Osaka City University, Sugimoto, Sumiyoshi-ku, Osaka 558-8585, Japan

[2] Ligand abbreviation: 3,6-Bu_2seq = 3,6-di-*tert*-butylsemiquinone, 3,6-Bu_2q = 3,6-di-*tert*-butylquinone,3,6-Bu_2cat = 3,6-di-*tert*-butylcatecholate, trpy = 2,2′:6′,2″-terpyridine, *o*-monothiocat = *o*-monothiocatecholato, *o*-monothioseq = *o*-monothiosemiquinone, *o*-monothioq = *o*-monothioquinone, bpy = 2,2′-bipyridine, 3,5-Bu_2seq = 3,5-di-*tert*-butylsemiquinone, 3,5-Bu_2q = 3,5-di-*tert*-butylquinone, cat = catecholato.

PII: S0022-328X(00)00941-4

hand, ruthenium(II)–polypyridyl–carbonyl complexes, $[Ru(CO)(bpy)(trpy)]^{2+}$, have been utilized as homogeneous catalysts in electrochemical reduction of CO_2, where electrons required in the reduction of CO_2 are provided by polypyridyl localized redox reactions [6]. It is, therefore, interesting to introduce a carbonyl ligand into ruthenium–polypyridyl–dioxolene complexes. Along the line, we have synthesized new complexes, $[Ru(CO)(o\text{-phenylene})(trpy)]^{n+}$ in which *o*-phenylene includes dioxolene and its mono-thio derivative, and found significant differences in chemical properties compared with those of $[RuX(o\text{-phenylene})(trpy)]^{n+}$ ($X = Cl^-$, CH_3COO^-, H_2O). The paper describes syntheses and properties of $[Ru(CO)(o\text{-phenylene})(trpy)]^{n+}$ and strong interactions between carbonyl and *o*-phenylene ligands.

2. Experimental

2.1. Materials

3,6-Di-*tert*-butylcatechol and *trans*-$[Ru(CO)Cl_2(trpy)]$ were prepared according to the reported method [7,8]. Tetra-*n*-butylammonium hexafluorophosphate ($TBAPF_6$) was used after twice recrystallization from hot ethanol. All other commercially available reagents were used as purchased.

2.2. Preparation of complexes

2.2.1. *[Ru(CO)(3,6-Bu_2seq)(trpy)]PF_6 ([**1**]PF_6)*

trans-$[Ru(CO)Cl_2(trpy)]$ (200 mg, 0.46 mmol), 3,6-di-*tert*-butylcatechol (102 mg, 0.46 mmol), and ^{t}BuOK (104 mg, 0.92 mmol) were suspended in 100 ml of 2-methoxyethanol. The mixture was refluxed for 3 h, during which time the suspension changed to a brown–green solution. After some precipitates were removed by filtration, the filtrate was concentrated under reduced pressure almost to dryness. The solid was dissolved in 10 ml of acetone and purified through an alumina column using acetone as an eluent. A blue component of $[Ru(CO)(3,6\text{-}Bu_2seq)(trpy)]Cl$ was separated first. The eluent was evaporated to 5 ml, and an addition of NH_4PF_6 (20 mg, 0.12 mmol) in a minimum amount of H_2O to the solution gave blue precipitate. Recrystallization of the crude product from acetone/ether afforded blue microcrystals of [**1**]PF_6, which were filtered off and air-dried. Yield 45 mg (14%). ESI-mass: *m*/*z* 583 ($\{M\}^+$), 363 ($\{M\text{-}3,6\text{-}Bu_2seq\}^+$). Anal. Found: C, 49.15; H, 4.49; N, 5.75. Calc. for $C_{30}H_{31}O_3N_3PF_6Ru$ (MW: 727.63): C, 49.52; H, 4.29; N, 5.77%. IR spectrum (KBr); *v*(CO) 1977 cm^{-1}.

2.2.2. *[Ru(CO)(3,6-Bu_2seq)(trpy)]BF_4 ([**1**]BF_4)*

To a solution obtained after column chromatography for [**1**]PF_6, $NaBF_4$ (10 mg, 0.12 mmol) in minimum of H_2O was added. Blue powder of [**1**]BF_4 was obtained, which was filtered off and air-dried. Yield 46 mg (15%). Anal. Found: C, 53.70; H, 4.76; N, 6.12. Calc. for $C_{30}H_{31}O_3N_3BF_4Ru$ (MW: 669.47): C, 53.82; H, 4.67; N, 6.28%.

2.2.3. *[Ru(CO)(o-monothiocat)(trpy)]·0.5H_2O*{2·0.5H_2O}

^{t}BuOK (104 mg, 0.92 mmol) was added to a mixture of *trans*-$[Ru(CO)Cl_2(trpy)]$ (200 mg, 0.46 mmol) and *o*-monothiocatechol (58 mg, 0.46 mmol) in 2-methoxyethanol (100 ml). The mixture was refluxed for 3 h and the resulting green solution was filtered to remove unsolved precipitate. The filtrate was evaporated to 10 ml and adsorbed on an alumina column. Using acetone as an eluent, brown band was separated first and collected. The solution was evaporated to 5 ml and allowed to stand for 1 day to give yellow–brown needle crystals. The crystals were filtered off and air-dried. Yield 25 mg (11%). ESI-mass: *m*/*z* 487 ($\{M\}^+$), 459 ($\{M\text{-}CO\}^+$). Anal. Found: C, 53.24; H, 3.36; N, 8.06. Calc. for $C_{22}H_{16}O_{2.5}N_3SRu$ (MW: 495.52): C, 53.33; H, 3.25; N, 8.48%. IR spectrum (KBr); *v*(CO) 1925, 1911, 1275 cm^{-1}.

2.3. Measurements

Cyclic voltammetry was performed with a BAS CV-100W voltammetry analyzer. Cyclic voltammograms were recorded at a scan rate of 50 mV s^{-1}. The sample solutions (ca. 1.0 mM) containing 0.1 M $TBAPF_6$ ($TBAPF_6$ = tetra *n*-butylammonium hexafluorophosphate) were deoxygenated in a stream of nitrogen gas. Redox potentials obtained were corrected by the potential of the ferrocenium/ferrocene couple. Electronic spectra were recorded on a Shimadzu UV–vis-NIR scanning spectrophotometer UV-3100PC. Spectroelectrochemical measurement was performed with a thin-layer electrode cell with a platinum mini grid working electrode sandwiched between two glass sides of an optical cell (the path length; 0.5 mm). ESR spectra were measured on a JEOL LES-FE2XG X-band spectrometer equipped with an Echo Electronics NMR field meter to calibrate the magnetic field and a Takeda Riken microwave counter TR5212 to obtain the microwave frequency, or a Bruker ESR-300E equipped with a Hewlett Packard microwave frequency counter 5352B. ^{1}H-NMR spectra were measured on a JEOL-EX 270 (270 MHz) spectrometer. IR spectra were obtained on a Shimadzu FTIR-8100 spectrophotometer.

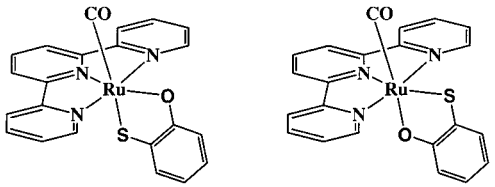

Fig. 1. Structures of two geometrical isomers of **2**.

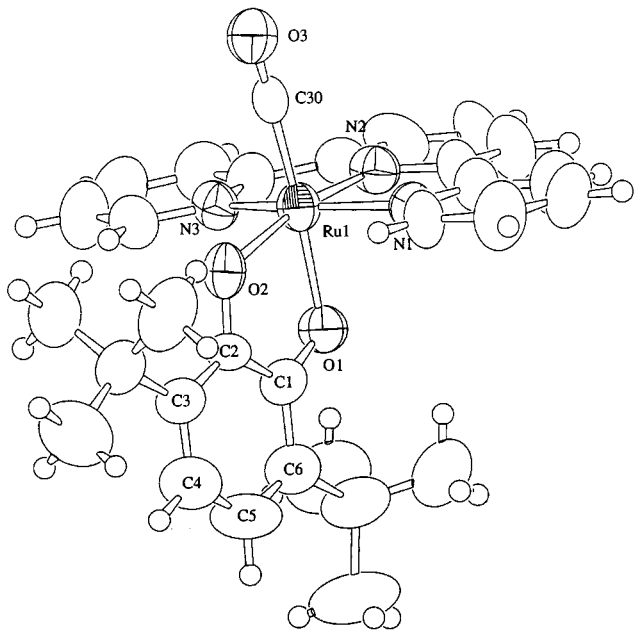

Fig. 2. Molecular structure of complex cation of [Ru(CO)(3,6-Bu_2seq)(trpy)]BF_4 ([**1**]BF_4) with the atomic numbering scheme showing 50% probability thermal ellipsoids.

2.4. X-ray crystallography

A single crystal of [**1**]BF_4 was obtained by slow diffusion of diethylether into an acetonitrile solution of the complex. A deep blue plate crystal of [**1**]BF_4 was attached on top of a glass fiber and the X-ray diffraction data were collected on a Siemens SMART/CCD diffractometer at 300 K. All the calculations were performed with the TEXSAN crystallographic software package [9]. The structure was solved by heavy-atom method and expanded using Fourier technique. All non-hydrogen atoms were refined anisotropically by full-matrix least-squares method. The hydrogen atoms were fixed at the calculated positions and not refined. Crystallographic data for [**1**]BF_4 is as follows: deep blue plate with $0.30 \times 0.15 \times 0.04$ mm; $C_{30}H_{31}O_3N_3BF_4Ru_1$; $a = 12.6966(8)$, $b = 11.8856(8)$, $c = 24.422(2)$ Å, $\beta = 91.01(1)°$, $V = 3684.9(4)$ Å^3; Mo–K_α: $\lambda = 0.71069$ Å; monoclinic; $P2_1/n$ (no. 14); $Z = 4$; Siemens SMART/CCD diffractometer; diffraction measurement method: omega scans with profile analysis; total number of data collected: 5351; 2θ limit = 50.0°; absorption correction was not applied; $R = 0.056$; $Rw = 0.058$; number of parameters: 379.

3. Results and discussions

3.1. Synthesis and characterization of complex

Monocarbonyl ruthenium polypyridyl complexes such as [Ru(CO)(bpy)(trpy)]$(PF_6)_2$ and [Ru(CO)$(bpy)_2$-(qu)]$(PF_6)_2$ (qu = quinoline) have been prepared by the reaction of the chloride analogs, [RuCl(bpy)(trpy)]PF_6 and [RuCl$(bpy)_2$(qu)]PF_6, with CO in the presence of $AgPF_6$, and utilized as homogeneous catalysts in electrochemical reduction of CO_2 [6,14]. On the other hand, a treatment of [RuCl(3,5-Bu_2seq)(trpy)] with $AgPF_6$ caused only the oxidation of the complex even under CO pressure, and CO was not incorporated into the complex. To avoid the oxidation of the complex, *o*-phenylenes were introduced to a monocarbonyl–ruthenium–terpyridyl complex. The reaction of *trans*-[Ru(CO)Cl_2(trpy)] with one equivalent of 3,6-di-*tert*-butylcatechol in 2-methoxy-ethanol gave monocationic deep blue [Ru(CO)(3,6-Bu_2seq)(trpy)]$^+$ ([**1**]$^+$), which was isolated as PF_6^- and BF_4^- salts ([**1**]PF_6 and [**1**]BF_4) in low yield (10–15%). Similar treatment of *trans*-[Ru(CO)Cl_2(trpy)] with *o*-monothiocatechol produced neutral yellow–brown [Ru(CO)(*o*-monothiocat)(trpy)] (**2**) in 11% yield. The complexes, [**1**]PF_6 and [**1**]BF_4, and **2**, were purified by alumina chromatography using acetone as an eluent. The IR spectrum of **2** displayed two strong ν(C=O) bands at 1925 and 1911 cm^{-1} with a peak intensity of ca. 1:1, indicating a mixture of two isomers due to the difference in the orientation of the chelate ring of *o*-monothiocatecholato (Fig. 1).

3.2. X-ray structure description of [1]BF_4

The crystal structure of cationic [**1**]$^+$ is shown in Fig. 2. The selected bond distances and angles are given in Table 1.

Ruthenium atom is coordinated with one carbonyl carbon, three nitrogen of terpyridine and two oxygen atoms of dioxolene ligand to take a distorted octahedral environment. The bond distances of 2.068(7), 1.977(7), and 2.075(7) Å between ruthenium and three nitrogen atoms in terpyridine are in the range of those of other ruthenium–terpyridine complexes, [Rupy-(bpy)(trpy)]$(PF_6)_2$ (py = pyridine, 2.078(7), 1.963(6), 2.079(7) Å) [10], [RuCl(bpz)(trpy)]PF_6 (bpz = 2,2′-bipyrazine, 2.068(2), 1.966(2), 2.077(2) Å) [11], [RuCl(H_2dppi)(trpy)]PF_6 (H_2dppi = 3,6-bis(pyrid-2-yl)pyridazine, 2.063(4), 1.952(4), 2.064(4) Å) [12], and [Ru(CO)(bpy)(trpy)]$(PF_6)_2$ (2.086(3), 1.988(3), 2.086(3) Å) [6]. The distance of Ru–C30 (C–O) of 1.850 (9) Å is

compared to that of $[Ru(CO)(bpy)(trpy)](PF_6)_2$ (1.844 (4) Å) [6].

Ruthenium dioxolene complexes are featured by close energy levels between 3d orbitals of Ru and π* orbitals of the ligands. Therefore, [**1**]BF_4 has three possible resonance isomers as depicted in Scheme 2 [3].

The contribution of each species is estimated by the C–O and C–C distances of dioxolene ligands. The bond distances at 1.283(9) and 1.301(8) Å of C1–O1 and C2–O2 of [**1**]BF_4, respectively, are close to one of the C–O distance of 1.289(14) Å of 3,5-di-*tert*-butylsemiquinone in $[Ru^{II}(bpy)_2(3,5\text{-}Bu_2seq)]ClO_4$, though somewhat shorter than the remaining C–O distance of 1.327(15) Å [4f]. Furthermore, the C–O distances of [**1**]BF_4 are compared to those of the average distance (1.30 Å) of two 3,6-di-*tert*-butylsemiquinone in $[Ru(CO)_2(3,6\text{-}Bu_2seq)_2]$ [13]. On the other hand, the C–O distances of [**1**]BF_4 are clearly shorter than those of 1.333(6) and 1.334(6) Å of catecholato in $[Ru(CH_3COO)(cat)(trpy)]$ [4], and the distances of 1.37(1), 1.36(1), 1.36(1), and 1.32(1) Å of 3,6-di-*tert*-butylcatecholato of $[Re^{V}(3,6\text{-}Bu_2cat)_2(trpy)]PF_6$ [7] having two *tert*-butyl groups on the same position as [**1**]BF_4. Based on these facts, the electronic structure of [**1**]BF_4 is denoted as $[Ru^{II}(CO)(3,6\text{-}Bu_2seq)(trpy)]BF_4$. However, slightly short C3–C4 and C5–C6 (1.35(1) and 1.36(1) Å), and slightly long C1–C2, C2–C3, C4–C5, and C1–C6 (1.43(1), 1.39(1), 1.43(1), and 1.43(1) Å, respectively) distances in [**1**]BF_4 suggest the contribution of the resonance form of $[Ru^{I}(3,6\text{-}Bu_2q)]BF_4$ in $[Ru^{II}(3,6\text{-}Bu_2seq)]BF_4$ (Scheme 2).

Table 1
Selected bond distances (Å) and angles (°) for [**1**]BF_4

Bond distances			
Ru1-O1	2.052(5)	Ru1-O2	2.062(5)
Ru1-N1	2.075(7)	Ru1-N2	1.977(7)
Ru1-N3	2.068(7)	Ru1-C30	1.850(9)
C1-C2	1.43(1)	C2-C3	1.39(1)
C3-C4	1.35(1)	C4-C5	1.43(1)
C5-C6	1.36(1)	C1-C6	1.43(1)
O1-C1	1.283(9)	O2-C2	1.301(8)
O3-C30	1.105(7)		
Bond angles			
O1-Ru1-O2	78.3(2)	O1-Ru1-N1	88.2(2)
O1-Ru1-N2	89.4(3)	O1-Ru1-N3	87.1(2)
O1-Ru1-C30	175.4(3)	O2-Ru1-N1	100.3(3)
O2-Ru1-N2	167.6(3)	O2-Ru1-N3	97.3(2)
O2-Ru1-C30	97.2(3)	N1-Ru1-N2	80.1(3)
N1-Ru1-N3	160.4(3)	N1-Ru1-C30	93.3(3)
N2-Ru1-N3	80.8(3)	N2-Ru1-C30	95.1(3)
N3-Ru1-C30	92.9(3)	Ru1-O1-C1	113.4(5)
Ru1-O2-C2	114.7(5)	Ru1-C30-O3	178.1(8)

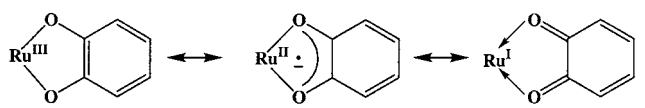

Scheme 2.

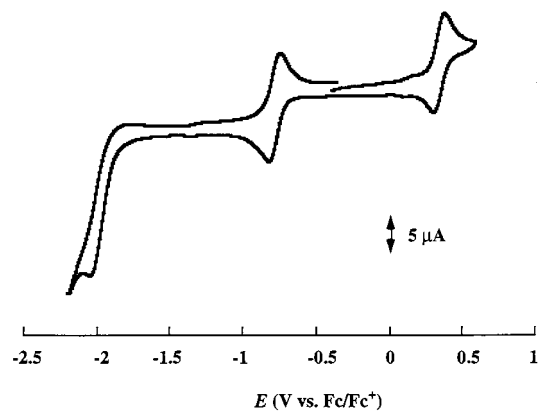

Fig. 3. Cyclic voltammogram of $[Ru(CO)(3,6\text{-}Bu_2seq)(trpy)]PF_6$ ([**1**]PF_6) in CH_2Cl_2 solution of $TBABF_4$ (0.1 M) at a glassy-carbon electrode with a scan rate of 50 mV s^{-1}.

3.3. Electrochemical properties

Both [**1**]PF_6 and **2** showed three redox couples in the cyclic voltammogram (CV) in the potential region of −2.5 to +1.0 V (versus Fc/Fc^+) in CH_2Cl_2. The CV of [**1**]PF_6 displayed reversible oxidation and reduction couples at $E_{1/2} = +0.33$ and −0.72 V, respectively, and an irreversible cathodic wave at −1.91 V (Fig. 3).

The neutral complex **2** underwent reversible oxidation and reduction at $E_{1/2} = -0.47$ and −1.88 V, respectively, and an quasi-reversible oxidation at $E_{pa} = +0.56$ (Table 2).

Taking into account that the trpy/$trpy^-$ redox reaction of an analogous $[RuCl(3,5\text{-}Bu_2seq)(trpy)]$ takes place at $E_{pc} = -2.10$ V [4], the redox couples near at −1.9 V of [**1**]PF_6 and **2** are reasonably associated with the terpyridyl localized redox reaction. The $[\mathbf{1}]^{2+/+}$ and $[\mathbf{1}]^{+/0}$ redox couples, therefore, are assigned to the dioxolene ligand localized (3,6-Bu_2-q/seq) and (3,6-Bu_2-seq/cat) redox couples, respectively. Similarly, two successive oxidations of the $[\mathbf{2}]^{0/+/2+}$ redox couples at $E_{1/2} = -0.47$ V and $E_{pa} = +0.56$ V are straightforwardly associated with the corresponding (*o*-monothioseq/cat) and (*o*-monothio-q/seq) ones, respectively. The difference in the redox potentials ($\Delta E \sim 250$ mV) between the $[\mathbf{1}]^{0/+/2+}$ redox couples and the corresponding $[\mathbf{2}]^{0/+/2+}$ ones are explained by strong electron donor ability of the dioxolene with di-*tert*-butyl groups compared with *o*-monothiocatecholato. The redox potentials of the (3,5-Bu_2-seq/cat) and (3,5-Bu_2-q/seq) couples in $[RuCl(3,5\text{-}Bu_2seq)(trpy)]$ are $E_{1/2} = -1.26$ and −0.37 V (versus Fc/Fc^+), respectively [4], and those in $[Ru(3,5\text{-}Bu_2seq)(bpy)_2]^+$ are $E_{1/2} = -0.91$ and −0.01 V (versus Fc/Fc^+) [4a], respectively. Thus, replacement of chloride of $[RuCl(3,5\text{-}Bu_2seq)(trpy)]$ by CO induced significant positive potential shift of the

Table 2
Electrochemical data of [Ru(CO)(3,6-Bu_2seq)(trpy)]PF_6 and [Ru(CO)(*o*-monothiocat)(trpy)] [a]

	$E_{1/2}$ [b] vs. Cp_2Fe^+/Cp_2Fe		
	trpy/trpy$^-$	*o*-phenylene$^-$/*o*-phenylene^{2-}	*o*-phenylene^0/*o*-phenylene$^-$
[Ru(CO)(3,6-Bu_2seq)(trpy)] [**1**]PF_6	−1.91	−0.72	+0.33
[Ru(CO)(*o*-monothiocat)(trpy)] [**2**]	−1.88	−0.47	+0.56
[RuCl(3,5-Bu_2seq)(trpy)] [c]	−2.10	−1.26	−0.37

[a] 3,6-Bu_2seq = 3,6-di-*tert*-butylsemiquinone, *o*-monothiocat = *o*-monothiocatecholato, 3,5-Bu_2seq = 3,5-di-*tert*-butylsemiquinone.
[b] $E_{1/2} = (E_{pa} + E_{pc})/2$, where E_{pa} and E_{pc} are anodic and cathodic peak potentials, respectively.
[c] Ref. [5].

redox potentials of the (3,5-Bu_2-seq/cat) and (3,5-Bu_2-q/seq) couples of [RuCl(3,5-Bu_2seq)(trpy)] by 540–700 mV, suggesting strong interaction between CO and the dioxolene ligand.

3.4. Electronic spectra

The electronic structure of [**1**]PF_6 is expected to show two MLCT bands: one is Ru(II) to 3,6-Bu_2seq and the other is Ru(II) to trpy. The former and the latter will disappear and remain, respectively, upon one electron reduction of the 3,6-Bu_2seq moiety of [**1**]PF_6. Indeed, [**1**]PF_6 showed strong electronic absorption bands at 388 and 625 nm in UV–vis region (a solid line in Fig. 4). Controlled potential electrolysis of [**1**]PF_6 at −1.0 V in CH_2Cl_2 resulted in a disappearance of the 388 and 625 nm bands, and a new band appears at 453 nm (a dotted line in Fig. 4). Based on the redox potentials of the (trpy/trpy$^-$) and the (3,6-Bu_2-seq/cat) couples, the bands at 388 nm and 625 nm of [**1**]PF_6 are assigned to the Ru(II) to trpy and Ru(II) to 3,6-Bu_2seq MLCT transitions, respectively, and the 453 nm band of [**1**]^0 is associated with the Ru(II) to trpy MLCT one. The red shift of the Ru(II) to trpy MLCT ($\Delta\lambda_{max} = 65$ nm) upon one electron reduction of 3,6-Bu_2seq in [**1**]PF_6 is explained by a rise of the energy levels of 3d orbitals of Ru(II).

Electronic spectrum of **2** showed an intense band at 404 nm assignable to the Ru(II) to trpy MLCT and no other strong absorption band was detected in visible region. One electron oxidation of **2** under the controlled potential electrolysis at 0.2 V in CH_2Cl_2 caused blue shift of the 404 nm band about by 40 nm, and the new MLCT band was observed as a shoulder overlapping with a strong ππ* aborption band of the ligands at 318 nm. In addition, MLCT band of the Ru(II) to *o*-phenylene in anion radical form of [**2**]$^+$ emerged at 658 nm in visible region. It is worthy of note that [Ru(3,5-Bu_2seq)(bpy)$_2$]PF_6 and [RuCl(3,5-Bu_2seq)(trpy)] display their Ru(II) to 3,5-Bu_2seq MLCT bands at 844 and 878 nm, respectively, and the one-electron oxidized forms, [Ru(3,5-Bu_2q)(bpy)$_2$]$^{2+}$ and [RuCl(3,5-Bu_2q)(trpy)]$^+$, showed the Ru(II) to 3,5-di-*tert*-butylquinone MLCT at 668 and 600 nm, respectively [4a]. In fact, strong CT bands around 600 and 850 nm of polypyridyl-Ru(II)-dioxolene complexes have been used as the criteria for the assignment of quinone and semiquinone forms. Accordingly, the 625 nm and 658 nm bands of [**1**]$^+$ and [**2**]$^+$, respectively, are close to those of polypyridyl-Ru(II)-quinone complexes rather than polypyridyl-Ru(II)-semiquinone ones reported so far [4a]. Significant high energy region of the Ru(II) to anion radical form of *o*-phenylene MLCT transitions of [**1**]$^+$ and [**2**]$^+$ also is indication of the strong interaction between carbonyl group and the *o*-phenylene ligands. In accordance with this, [Ru(CO)$_2$(3,6-Bu_2seq)$_2$] exhibits the Ru(II) to 3,6-Bu_2seq MLCT band at 970 nm [13].

3.5. Electronic states of complexes

The ESR of [**1**]PF_6 in CH_2Cl_2 at 4K showed a signal at $g = 2.00$ with peak to peak separation of about 35 G, and the pattern was reasonably explained by the presence of semiquinone ligand with a nearly free anion radical. The neutral **2** was ESR silent. In metal–dioxolene complexes, ν(C–O) bands of dioxolenes are also useful criteria for the estimation of the oxidation states; catecholato, semiquinone and quinone forms usually

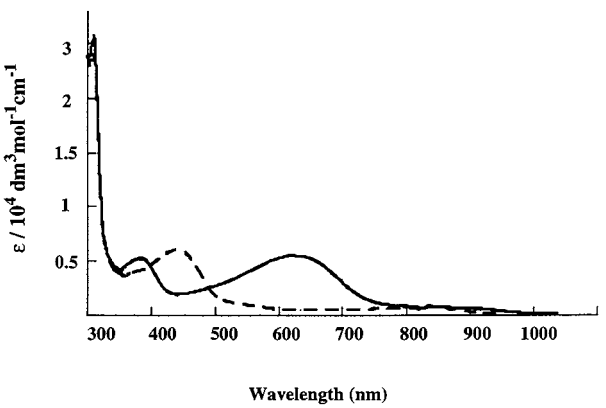

Fig. 4. Absorption spectra of [Ru(CO)(3,6-Bu_2seq)(trpy)]PF_6 ([**1**]PF_6) (solid line) and [Ru(CO)(3,6-Bu_2cat)(trpy)] [**1**] (dashed line) in CH_2Cl_2.

display their ν(C–O) bands near 1200 cm^{-1}, in the range of 1400–1500 cm^{-1}, and around 1600 cm^{-1}, respectively [3]. Although the ν(C–O) band in [**1**]PF_6 is not assigned unambiguously, it is safe to conclude that a strong band at 1275 cm^{-1} of **2** is correlated with the ν(C–O) band of catecholato. Thus, the ESR and IR spectra of [**1**]PF_6 and **2** also indicate their electronic structures as $[Ru^{II}(CO)(3,6\text{-}Bu_2seq)(trpy)]^+$ and $[Ru^{II}(CO)(o\text{-monothiocat})(trpy)]$, respectively.

The electrochemical reduction of [**1**]PF_6 at -1.0 V in CH_2Cl_2 caused the red shift of the ν(CO) band from 1977 to 1922 cm^{-1} ($\Delta\nu(CO) = -55$ cm^{-1}). On the other hand, one- and two-electron reductions of $[Ru(CO)(bpy)_2(quinoline)](PF_6)_2$ under the electrolysis at -1.21 and -1.50 V (versus Ag/AgCl) in CD_3CN shifted the ν(CO) band from 2015 cm^{-1} to 1980 and 1939 cm^{-1}, respectively [14]. The red shift of the ν(CO) band caused by the reduction of polypyridyl ligands of $[Ru(CO)(bpy)_2(quinoline)](PF_6)_2$ ($E_{1/2} = -1.11$ and -1.37 V) was less than -40 cm^{-1} per one electron. Thus, the unusual observation that the redox reaction of the (seq/cat) couple of [**1**]PF_6 at $E_{1/2} = -0.72$ V gave more serious effects on the back bonding from Ru(II) to CO than that of polypyridyl ligands of $[Ru(CO)(bpy)_2(quinoline)](PF_6)_2$ at $E_{1/2} = -1.11$ V is also implication of the strong interaction between carbonyl and dioxolene ligands compared with that of carbonyl and polypyridyl ligands.

4. Supplementary material

Crystallographic data (excluding structure factors) for the structure in this paper have been deposited with the Cambridge Crystallographic Data Centre CCDC no. 150987. Copies of this information may be obtained free of charge from The Director, CCDC, 12 Union Road, Cambridge CB2 1EZ, UK (Fax: +44-1223-336033; e-mail: deposit@ccdc.cam.ac.uk or www: http://www.ccdc.cam.ac.uk).

Acknowledgements

The authors are grateful to Professor Makoto Fujita (Nagoya University) for collection of X-ray data, to Professor Yoshihito Watanabe and Dr Seiji Ogo for assistance in ESI-MS measurements.

References

[1] (a) C.G. Pierpont, C.W. Lange, Prog. Inorg. Chem. 41 (1994) 331. (b) C.G. Pierpont, R.M. Buchanan, Coord. Chem. Rev. 38 (1981) 35.
[2] (a) M. Muratalie, M. Klein, A. Fulco, R. Feyereisen, Biochemistry 36 (1997) 8401. (b) G.L. Closs, J.R. Miller, Science 240 (1988) 440. (c) S. Baez, J. Sequra-agular, M. Wildersten, A. Johansson, B. Mannervik, Biochem. J. 324 (1997) 25.
[3] (a) M. Haga, E.S. Dodsworth, A.B.P. Lever, Inorg. Chem. 25 (1986) 447. (b) H. Masui, A.B.P. Lever, P.R. Auburn, Inorg. Chem. 30 (1991) 2402. (c) C.J. da Cunha, S.S. Fielder, D.V. Stynes, H. Masui, P.R. Auburn, A.B.P. Lever, Inorg. Chim. Acta. 242 (1996) 293. (d) S. Bhattacharya. S.R. Boone, G.A. Fox, C.G. Pierpont, J. Am. Chem. Soc. 112 (1990) 1088. (e) M. Haga, K. Isobe, S.R. Boone, C.G. Pierpont, Inorg. Chem. 29 (1990) 3795. (f) S.R. Boone, C.G. Pierpont, Inorg. Chem. 26 (1987), 1769.
[4] M. Kurihara, S. Daniele, K. Tsuge, H. Sugimoto, K. Tanaka, Bull. Chem. Soc. Jpn. 71 (1998) 867.
[5] K. Tsuge, M. Kurihara, K. Tanaka, Bull. Chem. Soc. Jpn. 73 (2000) 607.
[6] H. Nagao, T. Mizukawa, K. Tanaka, Inorg. Chem. 33 (1994) 3415.
[7] H. Sugimoto, K. Tsuge, K. Tanaka, Chem. Lett. (1998) 718.
[8] G.B. Deacon, L.M. Patrick, B.W. Skelton, N.C. Thomas, A.H. White, Aust. J. Chem. 37 (1984) 929.
[9] TEXSAN, Single Crystal Structure Analysis Package. Molecular Structure Corporation: The Woodlands, TX 77381, USA, 1992.
[10] C.R. Hecker, P.E. Fanwick, D.R. McMillin, Inorg. Chem. 30 (1991) 659.
[11] A. Gerli, J. Reedijk, M.T. Lakin, A.L. Speck, Inorg. Chem. 34 (1995) 1836.
[12] V.J. Catalano, R.A. Heck, C.E. Immoos, A. Ohman, M.G. Hill, Inorg. Chem. 37 (1998) 2150.
[13] S. Bhattacharya, C.G. Pierpont, Inorg. Chem. 33 (1994) 6038.
[14] H. Nakajima, Y. Kushi, H. Nagao, K. Tanaka, Organometallics 14 (1995) 5093.